JOURNAL OF Materials CHEMISTRY

A novel procedure for the synthesis of NH_3 incorporated VPO phases

Arunabha Datta,* Monika Agarwal and Soumen Dasgupta

Indian Institute of Petroleum, Dehra Dun 248 005, India. E-mail: adatta@iip.res.in; Fax: 91-135-660202, 660203; Tel: 91-135-660263(O), 660119(R)

Received 16th January 2002, Accepted 18th March 2002
First published as an Advance Article on the web 25th April 2002

It has been observed that as a function of a time delay introduced between the onset of the reduction of V_2O_5 with hydroxylamine hydrochloride and the addition of phosphoric acid, in the aqueous route preparation of the catalytically important $VOHPO_4{\cdot}0.5H_2O$ phase, a series of NH_3 incorporated phases are obtained. Up to delay times of 3 min the crystalline $VOHPO_4{\cdot}0.5H_2O$ phase is obtained whereas a weakly crystalline hemihydrate is formed at a delay time of 4 min. Longer delay times result in X-ray amorphous phases until at delay time of 10 min and above a new crystalline phase containing mixed-valent vanadium emerges. All the phases obtained with delay times of 4 min and above have NH_3 incorporated into them. The weakly crystalline $VOHPO_4{\cdot}0.5H_2O$ phase as well as the X-ray amorphous phases undergo transformation to a crystalline vanadyl pyrophosphate phase on calcination at 723 K in spite of having NH_3 incorporated into them. The *in-situ* generation of NH_3 during the preparation procedure is a hitherto unreported aspect of VPO chemistry and provides a convenient method for the preparation of novel NH_3 incorporated VPO phases which could have strong potential as catalysts for alkane oxidation as well as for ammoxidation reactions.

Introduction

The vanadium phosphates offer a wide variety of structural modifications both because of the variable oxidation state of vanadium and because of the different ways in which the vanadium octahedra and the phosphate tetrahedra can be linked together to give extended layered structures.[1] The vanadium orthophosphate hemihydrate $VOHPO_4{\cdot}0.5H_2O$ is important as the precursor for the $(VO)_2P_2O_7$ catalyst used industrially in the selective oxidation of butane to maleic anhydride.[1,2] This is a structure sensitive reaction in which the activity of the catalyst is strongly dependent upon its morphology and physico-chemical characteristics. The active pyrophosphate phase is obtained from the hemihydrate precursor through a topotactic transformation and consequently changes incorporated in the precursor are retained in the active phase after transformation.[2]

Conventionally the precursor is prepared by the reduction of V_2O_5 in either aqueous[3] or organic[4] medium using $NH_2OH{\cdot}HCl$ or isobutanol–benzyl alcohol mixture respectively as the reductant followed by the addition of a stoichiometric amount of H_3PO_4. More recently it has been reported[5] that higher selectivity to maleic anhydride can be achieved by synthesizing the precursor starting from $VOPO_4{\cdot}2H_2O$ rather than V_2O_5. The higher activity has been attributed to the larger surface area of the precursor and eventually of the active phase when synthesized starting from $VOPO_4{\cdot}2H_2O$. It has also been demonstrated[6] that the best activity for oxidation of butane to maleic anhydride was obtained with a vanadyl pyrophosphate catalyst which had V^{4+} ions in a crystalline matrix in addition to a disordered matrix containing both V^{4+} and V^{5+}. In fact, the specific activity of the catalysts increases with increasing concentration of V^{4+}–V^{5+} dimers. Such mixed valent phases have been found to catalyze not only the oxidation of butane to maleic anhydride but are also active in ammoxidation processes.[7] It has in general been observed that the presence of V^{5+} is desirable, since the oxygen associated with them is more labile and active in oxygen insertion steps.[8]

In our previous work[9] we have demonstrated that the incorporation of metal ions has a pronounced effect on the structure, morphology, oxidation state of vanadium and the catalytic activity of the vanadium phosphates. In the present work we report the formation of a series of phases and the ultimate emergence of a new mixed valent vanadium phosphate phase by modifying the procedure for the preparation of $VOHPO_4{\cdot}0.5H_2O$ involving the reduction of V_2O_5 in aqueous medium. It has been observed that by introducing a time interval between the onset of the reduction of V_2O_5 with hydroxylamine hydrochloride and the addition of phosphoric acid, a series of NH_3 incorporated vanadium phosphate phases are formed as a function of the time delay.

Experimental

In the reported preparation[3] of $VOHPO_4{\cdot}0.5H_2O$, typically 1.818 g of V_2O_5 was mixed with 2.30 g of 85% phosphoric acid and 1.4 g $NH_2OH{\cdot}HCl$ in water and heated to 353 K for 1 h. The blue homogeneous solution was then evaporated to dryness and heated overnight to 393 K. However the above procedure was modified by heating the slurry of V_2O_5 and hydroxylamine hydrochloride to 353 K and then adding the requisite amount of H_3PO_4 **after a time interval** of 0, 1, 2, 3, 4, 5, 6, 7, 8, 9, 10 & 30 min. The final phases were then isolated in the usual manner as described above in the preparation of $VOHPO_4{\cdot}0.5H_2O$. The phases obtained at different delay times are referred to as **P-0**, **P-1**, **P-2**, **P-3**, **P-4**, **P-5**, **P-6**, **P-7**, **P-8**, **P-9**, **P-10** and **P-30** respectively.

The X-ray powder diffractograms were recorded on a GE XRD 9530 diffractometer using CuKα radiation (λ = 1.5406 Å). FTIR spectra were recorded on a Perkin Elmer 1760x FTIR spectrometer with the sample powder diluted in KBr (1%). Typically 100 scans with a resolution of 4 cm^{-1} were collected for each sample. UV-VIS spectra were recorded on a Perkin Elmer λ 19 model spectrometer using MgO as the reference. X-ray photoelectron spectra were obtained on powdered samples with a FISONS system using monochromated MgKα radiation (1253.6 eV). For energy referencing the C_{1s} line (BE at 285 eV) was used. Thermogravimetric analysis was carried out using a Mettler TG50 model at

 DOI: 10.1039/b200562j

a heating rate of 283 K min^{-1} under a nitrogen flow of 150 ml min^{-1}. An Hitachi S. 2460N scanning electron microscope was employed to obtain topographical information from the specimens. The average oxidation state was determined by redox titration wherein about 0.1 g of the compound was dissolved in 2 mol dm^{-3} H_2SO_4 (100 cm^3) at 353 K. The vanadium(IV) content was then determined by titration (V_1) with 0.1 mol dm^{-3} $KMnO_4$ and the vanadium(V) content by titration (V_2) with 0.1 mol dm^{-3} ammonium iron(II) sulfate using diphenylamine as indicator. The average oxidation state was then expressed as $5 - (V_1/V_2)$.

Results

XRD

The XRD patterns of the different phases obtained as a function of the delay time (Fig. 1) show that the phases **P-0** to **P-3** correspond[4] to that of pure $VOHPO_4{\cdot}0.5H_2O$ although the lines in the XRD pattern of **P-3** are broader indicating a reduction in long range order. Also the relative intensities of some of the lines are different. The XRD patterns of **P-1** and **P-2** are not shown since they are identical to that of **P-0**. The XRD pattern of **P-4** shows lines due to the $VOHPO_4{\cdot}0.5H_2O$ phase superimposed on a very broad peak suggesting the presence of an additional amorphous phase. The phases **P-5** and **P-6** on the other hand are X-ray amorphous. At 7 min delay time a new crystalline phase **P-7** appears which becomes more ordered when delay times of 8, 9 & 10 min are employed. The XRD pattern of this phase (**P-10**) is completely different from that of $VOHPO_4{\cdot}0.5H_2O$ or any of the other known phases in the VPO system. Also, this phase remains unchanged even when delay times of up to 30 min (**P-30**) are used. This phase with a basal spacing of 6.8 Å shows predominant ordering along the *c*-axis and the XRD pattern though drastically different from that of $VOHPO_4{\cdot}0.5H_2O$ bears a close resemblance to that of the metal intercalates of the $VOPO_4{\cdot}2H_2O$ phase.[10]

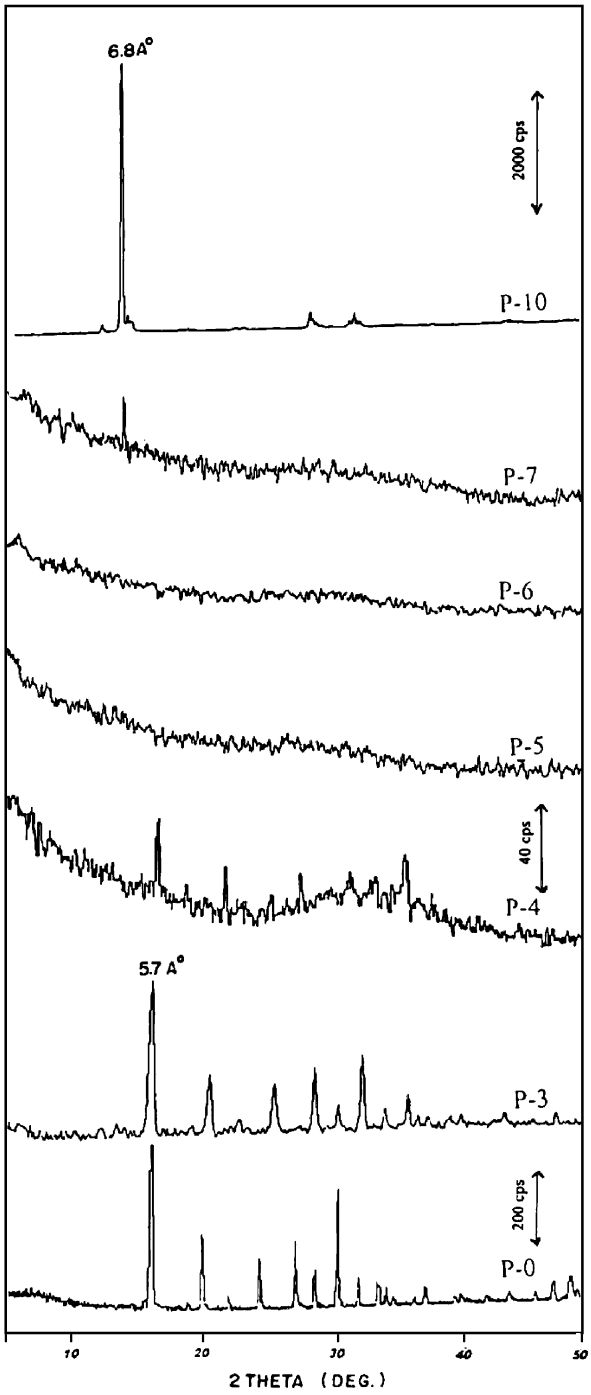

Fig. 1 XRD patterns of phases prepared with different delay times.

FTIR

The FTIR spectra (Fig. 2a & 2b) corroborate the XRD data, with the spectra of the phases **P-0** to **P-3** corresponding to that reported[4] for $VOHPO_4{\cdot}0.5H_2O$. A sharp band at 3368 cm^{-1} in the O–H stretching region in the phases **P-0** & **P-3** is due to the stretching vibration of structural H_2O bound to two vanadium(IV) in the face shared dioctahedra of VO_6 units in the $VOHPO_4{\cdot}0.5H_2O$ lattice. The bending mode of this bridgehead positioned H_2O (V–OH_2–V) is visible as a relatively broad

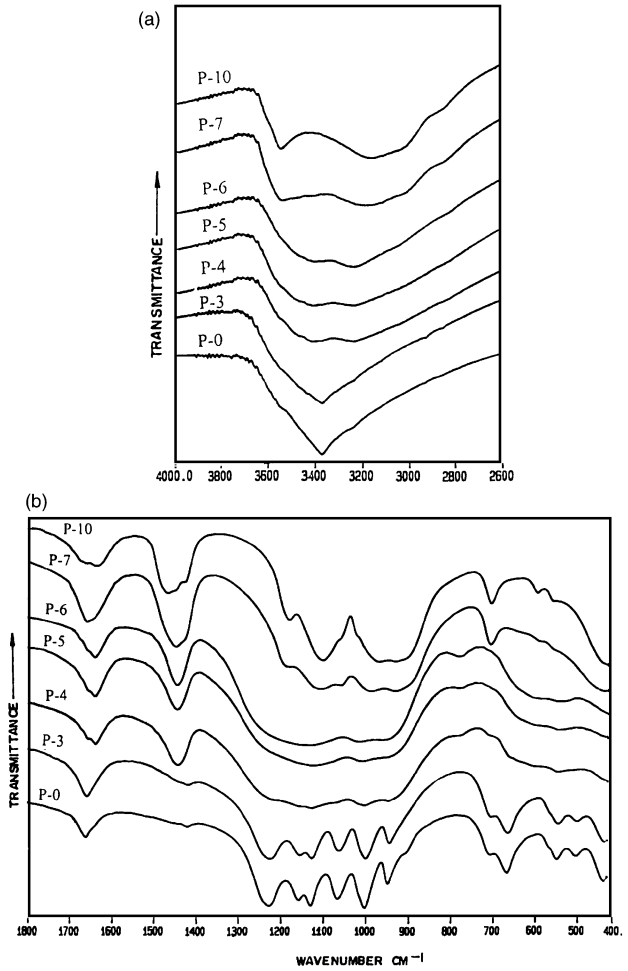

Fig. 2 (a) FTIR spectra of phases prepared with different delay times (O–H stretching region); (b) FTIR spectra of phases prepared with different delay times (P–O, V–O stretching region).

band centered at 1640 cm^{-1}. Interestingly, the onset of disorder in the $VOHPO_4{\cdot}0.5H_2O$ phase observed in **P-4** and the subsequent formation of the X-ray amorphous phases **P-5** and **P-6** are associated with the appearance of bands at 3234 cm^{-1} and at 1610 & 1425 cm^{-1} which correspond[11] to the N–H stretching (3234 cm^{-1}) and bending modes of NH_3 bound to Lewis (1610 cm^{-1}) and Bronsted (1425 cm^{-1}) acid sites respectively. In addition there are bands at 3375 cm^{-1} and a shoulder at 1640 cm^{-1} due to $VOHPO_4{\cdot}0.5H_2O$ suggesting thereby that **P-4**, **P-5** and **P-6** contain the $VOHPO_4{\cdot}0.5H_2O$ phase with NH_3 incorporated into it or an additional phase with bound NH_3 species. However, on the appearance of a crystalline new phase **P-10**, the OH stretching region is dominated by bands at 3546 cm^{-1} and 3164 cm^{-1}. This is also associated with the reappearance of a strong band at 1640 cm^{-1} due to the bending mode of water along with bands at 1615 cm^{-1} and at 1444 cm^{-1} and 1410 cm^{-1}. Out of these, the band at 1615 cm^{-1} can be assigned to NH_3 bound to Lewis acid sites whereas the bands at 1444 cm^{-1} and 1410 cm^{-1} are reported[11] to be due to NH_3 bound to Bronsted acid sites of the type P–OH and V–OH respectively. It is to be noted here that the bands due to the bound NH_3 species in **P-10** are different from those observed in **P-4**, **P-5** & **P-6**. In essence it is apparent that the presence of bound NH_3 causes the loss in crystallinity of the initially formed $VOHPO_4{\cdot}0.5H_2O$ and the subsequent formation of an amorphous phase. The eventual formation of a crystalline new phase **P-10** is also associated with bound NH_3 species though of a different nature. The spectrum of **P-10** in the P–O, V–O stretching region is suggestive of mixed valency of vanadium with bands at 1035 cm^{-1} and 997 cm^{-1} which can be assigned[10] to the V^{v}=O and V^{iv}=O stretching frequencies.

TPR

The TPR profiles of the samples prepared with different delay times (Fig. 3) indicate that sample **P-0** has only one reduction peak at 1033 K in agreement with the earlier reported[12] peak for $VOHPO_4{\cdot}0.5H_2O$ corresponding to the reduction of V^{4+} to V^{3+} species. In the case of **P-4** however, in addition to the peak at 1033 K another broad peak centered at 807 K is observed which can be ascribed to the reduction of V^{5+} to V^{4+} species. In samples **P-5** and **P-6**, broad peaks are observed at 763 K and 1013 K due to the reduction of V^{5+} and V^{4+} species respectively. The broadness of the peaks corroborates the amorphous nature of these samples indicated by XRD data. At the same time, the fact that the reduction temperature of the V^{4+} species in these samples is fairly close to that of $VOHPO_4{\cdot}0.5H_2O$ would seem to suggest that the phase present in **P-5** and **P-6**, though amorphous, is similar to that of the hemihydrate. In the case of **P-10**, however two very well defined peaks are observed at 743 K and 1033 K which can be attributed to the reduction of V^{5+} & V^{4+} species respectively, suggesting thereby the presence of a mixed valent vanadium phosphate phase in **P-10**.

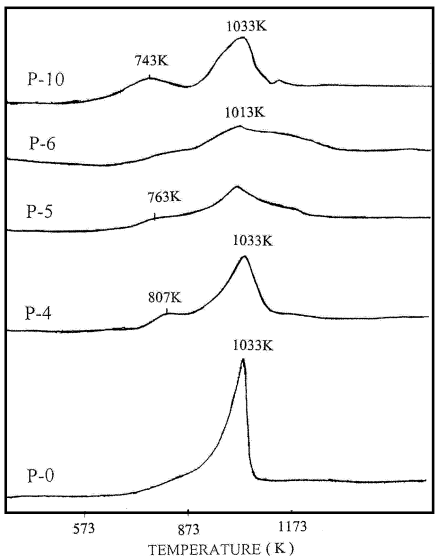

Fig. 3 TPR profiles of phases with different delay times (**P-0**, **P-4**, **P-5**, **P-6**, **P-10**).

SEM

The SEM micrographs (Fig. 4) show that **P-0** has a platelet structure with sizes ranging in diameter from 20–30 μm. The platelets are irregular shaped and randomly clustered. **P-4** also has a platelet structure with platelets varying widely in size. On the other hand although **P-5** also has a platelet morphology, the platelets are randomly clustered together and not as distinctly separated as in **P-4**. In contrast to the other three samples, **P-10** has a well formed morphology which consists of platelets of a fairly uniform size of around 8–10 μm, clustered together. The platelet size is much smaller and more uniform than that of the others. The well defined morphology of **P-10** is in agreement with its crystalline nature.

It is evident therefore that as a function of delay time introduced between the reduction of V_2O_5 and the addition of phosphoric acid, a whole range of phases are obtained starting with the $VOHPO_4{\cdot}0.5H_2O$ phase and passing through amorphous phases **P-5** and **P-6** to a new crystalline phase **P-10**. The formation of the new phase is first evident in **P-7** and becomes crystalline through **P-8** and **P-9** up to **P-10**. The structure remains invariant when delay times of over 10 min are used. Consequently **P-10** was taken as representative of the new phase and was characterized in more detail.

Characterization of P-10

The analysis of **P-10** was found to correspond to the composition $VOPO_{4{\cdot}02}H_{0.44}(NH_3)_{0.51}{\cdot}1.8H_2O$. The average oxidation state of vanadium as determined by redox titration in **P-10** was found to be +4.65, indicating mixed valency.

The XPS of **P-10** (Fig. 5) provides further evidence for the presence of mixed valent vanadium. The broad peak due to the $V_{2p_{3/2}}$ state can be resolved into two components due to V^{5+} and V^{4+} species with binding energies (BE) of 518.0 eV and 516.9 eV respectively. On the other hand the presence of

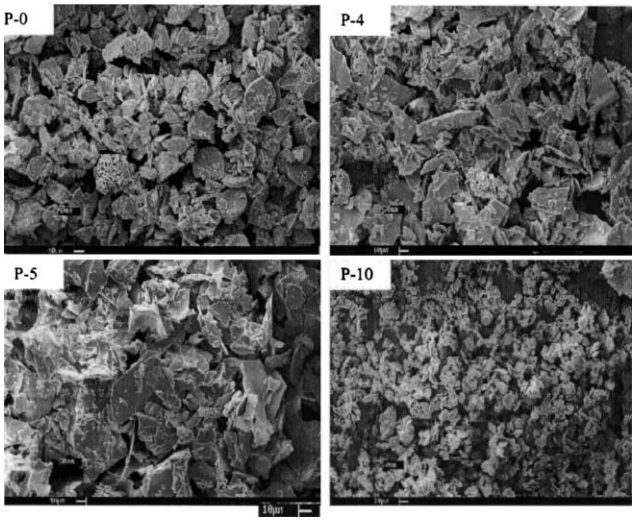

Fig. 4 Scanning electron micrographs of phases with different delay times (**P-0**, **P-4**, **P-5**, **P-10**).

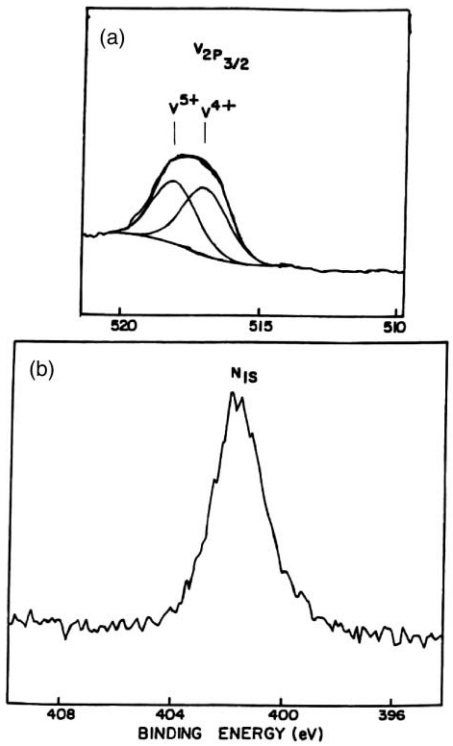

Fig. 5 XPS of **P-10** (a) $V_{2p_{3/2}}$ and (b) N_{1s} region.

a peak at 401.6 eV suggests the presence of NH_4^+ type species in **P-10** as is also indicated in the infrared spectrum.

The UV-visible reflectance spectrum (Fig. 6) of **P-10** shows strong bands at 420 & 330 nm and a weaker broad band centered at 740 nm. The spectrum of $VOPO_4{\cdot}2H_2O$ has strong bands at 330 nm and 420 nm which have been assigned[13] to charge transfer transitions from lattice oxide to V^{5+} species, in tetrahedral and octahedral environments respectively. On the other hand, the spectrum of $VOHPO_4{\cdot}0.5H_2O$ shows a strong band at 260 nm which has been ascribed to a charge transfer band arising from electron transfer between oxygen and vanadium ions.[14] In addition there are absorption bands at 640 nm and 820 nm which have been assigned to the $2B_2 \rightarrow 2B_1$ and $2B_2 \rightarrow 2E_1$ transitions of V^{4+} ions in a distorted octahedral symmetry. Consequently the bands at 330 nm and 420 nm in the case of **P-10** can be attributed to charge transfer transitions involving V^{5+} species, in tetrahedral and octahedral co-ordination respectively. On the other hand, unlike in the case of $VOHPO_4{\cdot}0.5H_2O$, no bands are observed at 640 nm and 820 nm. Instead a stronger broad band at 740 nm is observed which can be assigned to charge transfer transition between V^{4+} and V^{5+} species. A similar assignment has been made by Flynn and Pope[15] of a band at 770 nm, observed in mixed valent decavanadate. In essence therefore the UV-visible reflectance studies provide further evidence for the presence of both V^{4+} & V^{5+} species in **P-10** and the presence of a band due to an intervalence transition indicates close proximity of the V^{4+} and V^{5+} ions.

The simultaneous DSC/TGA pattern (Fig. 7) of **P-10** in a nitrogen atmosphere indicates weight loss of 8.5% and 7.8% at peak temperatures of 350 K and 473 K respectively and the DSC pattern also shows endothermic peaks corresponding to these temperatures. This weight loss can be ascribed, in conjunction with infrared data, to the loss of water molecules held in the interlayer and bound to the lattice respectively. In addition there is a broad weight loss of 5.5% in the region 513–773 K and centered at 613 K which can be ascribed to the loss of ammonia bound to **P-10**. The weight loss of 5.5% in the temperature range 513–773 K is however higher than the total ammonia present as derived from nitrogen content. This suggests the probable loss also, in this temperature range, of some water molecules through condensation of P–OH groups present in **P-10**. The FTIR spectrum of **P-10** heated in nitrogen atmosphere at 773 K for 1 h did not show the presence of bands in the 1615 cm^{-1} and 1440–1410 cm^{-1} regions due to bound ammonia species and the calcined sample was also found to be X-ray amorphous.

The EPR spectrum (Fig. 8) of **P-10** shows a sharp signal with a peak width of 30 G centered at $g_1 = 1.9708$ overlapping a broader signal with $g_2 = 1.9574$, thus indicating the presence of two types of V^{4+} ions with different environments. The spectrum of $VOHPO_4{\cdot}0.5H_2O$ on the other hand shows a broad isotropic signal[16] (line width 80 G) with a g value of 1.9618. The presence of two different V^{4+} environments in **P-10** is in keeping with the presence of both V^{4+} and V^{5+} species as indicated by other studies. The narrower signal ($g_1 = 1.9708$) would correspond to V^{4+} ions in the vicinity of V^{5+} species with the narrowing of the signal being due to a less efficient relaxation process between the V^{4+} paramagnetic centers shielded by V^{5+} ions.

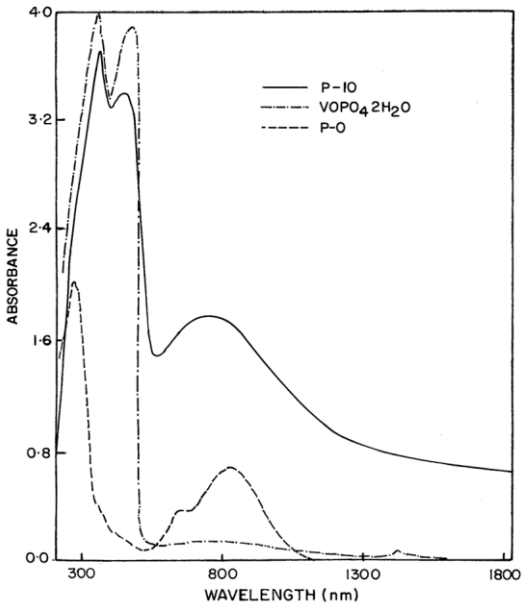

Fig. 6 UV-visible reflectance spectra of **P-0**, **P-10** and $VOPO_4{\cdot}2H_2O$.

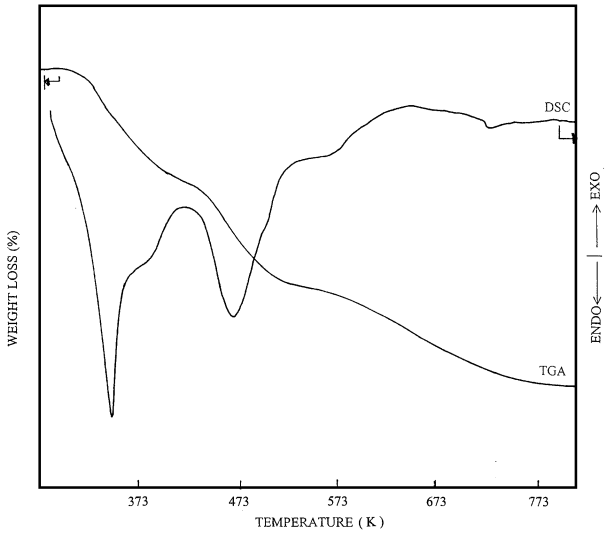

Fig. 7 Simultaneous DSC/TGA of **P-10** (heating rate 283 K min^{-1} and nitrogen flow of 150 ml min^{-1}).

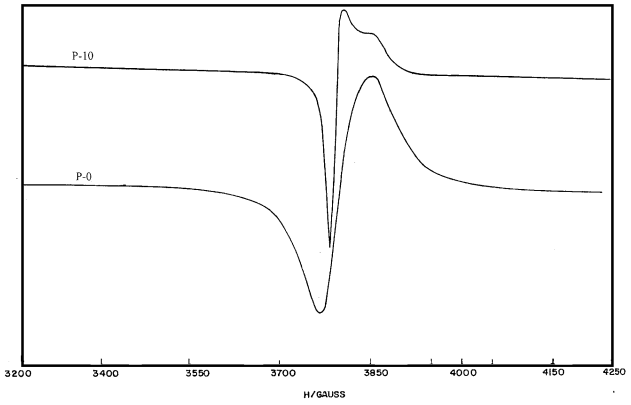

Fig. 8 EPR spectra (at RT) of $VOHPO_4{\cdot}0.5H_2O$ and **P-10**.

Discussion

It is evident therefore that by introducing a delay between the start of the reduction of V_2O_5 and the addition of H_3PO_4, a range of vanadium phosphate phases can be obtained starting from the $VOHPO_4{\cdot}0.5H_2O$ phase to a new mixed-valent phase. It is also apparent that the presence of NH_3 generated during the reactions plays an important role in deciding the structure of the phases formed.

The formation of NH_3 from the hydroxylamine hydrochloride is itself a novel and intriguing aspect of the chemistry of VPO compounds. In the normal preparation of $VOHPO_4{\cdot}0.5H_2O$ where there is no time delay between the commencement of the reduction of V_2O_5 and the addition of phosphoric acid, the V^{4+} produced is immediately consumed by the phosphoric acid thereby shifting the equilibrium of the reaction to the right, and facilitating the further reduction of V_2O_5. However, with a delay in the addition of phosphoric acid there would be an accumulation of V^{4+} species in solution. It would appear that up to delay times of 3 min, the concentration of V^{4+} species does not cause any deviation from the usual route leading to the formation of the $VOHPO_4{\cdot}0.5H_2O$ phase. However, for delay times of 4 min and above it is obvious that formation of NH_3 takes place since all the phases **P-4** to **P-10** show clear evidence for the presence of bound NH_3 species. This strongly suggests that on accumulation of V^{4+} species the N^{1-}/N^{3-} couple ($E^\circ = +1.35$ V) of $NH_2OH{\cdot}HCl$ is activated which oxidises V^{4+} to V^{5+} ($E^\circ = -0.957$ V) and generates NH_3 in the process. At the time of the addition of H_3PO_4 after a delay time of 4 min both V^{4+} & V^{5+} species should be present in solution and consequently one would expect a mixture of both V^{4+} and V^{5+} phases to be formed. That this indeed is the case is evident from the average vanadium oxidation state of +4.1 for **P-4** and from the TPR pattern which shows peaks due to the reduction of both V^{5+} and V^{4+} species. This in conjunction with its XRD pattern suggests that **P-4** is a mixture of the crystalline $VOHPO_4{\cdot}0.5H_2O$ phase and an X-ray amorphous V^{5+} phase. This is also evident from the FTIR spectrum of **P-4** which shows a band at 1132 cm^{-1} due to the P–OH stretch of the pure $VOHPO_4{\cdot}0.5H_2O$ phase. It has been observed[17] earlier that penetration of NH_3 into the layers of $VOHPO_4{\cdot}0.5H_2O$ makes it amorphous due to the interaction of the NH_3 with the P–OH groups of the hemihydrate and consequently the presence of a band at 1132 cm^{-1} clearly indicates that there is no interaction of NH_3 with the $VOHPO_4{\cdot}0.5H_2O$ component of **P-4**. At the same time the broadening out of the P–O, V–O stretching region of **P-4** suggests the presence of an amorphous phase. The V^{5+} phase present in **P-4** is amorphous probably due to its interaction with NH_3 as has been reported earlier.[17] Phases **P-5** and **P-6** are X-ray amorphous, indicating that the crystalline $VOHPO_4{\cdot}0.5H_2O$ component of **P-4** had also now become amorphous due to the incorporation of NH_3 species. Evidence for this is provided by the observation that the P–OH stretching frequency is shifted to 1104 cm^{-1} in **P-6** due to interaction with NH_3.

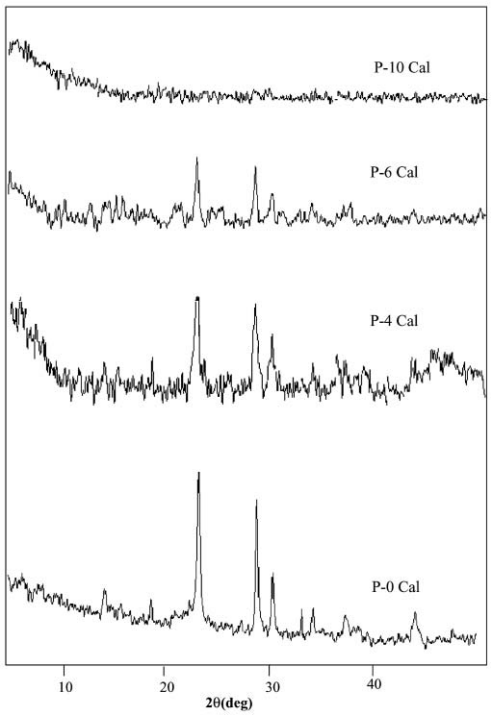

Fig. 9 XRD patterns of **P-0**, **P-4**, **P-6** and **P-10** calcined under N_2 atmosphere at 723 K.

The XRD patterns (Fig. 9) of **P-0**, **P-4**, **P-6** and **P-10** calcined at 723 K in N_2 show that **P-4** and **P-6** like **P-0** also undergo transformation to the crystalline pyrophosphate phase while **P-10** gives rise to an amorphous phase. The formation of a crystalline pyrophosphate phase from the amorphous **P-6** phase indicates that on heating, the bound NH_3 species are released and the P–OH groups of the orthophosphate are freed allowing them to undergo condensation to the pyrophosphates.

It was observed that during the preparation of all samples up to **P-6**, a clear solution was observed after addition of phosphoric acid, whereas in the case of **P-7** to **P-10**, all the V_2O_5 does not go into solution and a slurry is formed. The undissolved solid from this slurry was isolated and its colour was found to be considerably darker than that of V_2O_5. Also the infrared spectrum of this sample after thorough washing with water showed bands at 1401 cm^{-1} and 1626 cm^{-1} in addition to those of V_2O_5. These additional bands can be ascribed to NH_4^+ type species and NH_3 bound to Lewis acid sites respectively. This indicates that the NH_3 liberated stabilizes the unreduced V_2O_5 thus permitting the formation of a mixed-valent phase containing both the V^{4+} and V^{5+} species.

From the detailed characterization of **P-10**, it is evident that it is a new mixed-valent crystalline VPO phase with incorporated NH_3 species. The similarity of the XRD pattern of **P-10** with that reported[10,18] for metal intercalates of $VOPO_4{\cdot}2H_2O$ would seem to suggest that **P-10** could be a phase containing NH_4^+ ions intercalated into the $VOPO_4{\cdot}2H_2O$ phase. However, the infrared spectrum of **P-10** clearly indicates the presence of NH_3 bound to Lewis and Bronsted acid sites rather then the presence of NH_4^+ ions. Of course, the interaction of NH_3 with Bronsted acid sites would also lead to the formation of NH_4-type species but the infrared bands at 1444 cm^{-1} and 1410 cm^{-1} in the spectra of **P-10** clearly indicate the presence of NH_3 bound to P–OH and V–OH moieties rather than the presence of NH_4^+ ions.

Moreover, the amorphous phases such as **P-6**, preceding the formation of **P-10** in the evolution process, have been shown to consist of NH_3 incorporated $VOHPO_4{\cdot}0.5H_2O$ phases since they undergo transformation to the pyrophosphate phase. Consequently the transition from a face sharing dimeric VO_6 octahedral structure as in $VOHPO_4{\cdot}0.5H_2O$ to a single octahedral structure as in $VOPO_4{\cdot}2H_2O$ with an increase in delay time from 6 to 10 min is most unlikely. In essence therefore, although complete structural details of **P-10** are not available since it has not been possible to grow single crystals of this phase, it is quite evident that **P-10** is a new, NH_3 incorporated phase in the VPO system containing mixed valent vanadium.

Conclusions

1. The present study demonstrates that by varying the delay time between the onset of reduction of V_2O_5 and the addition of phosphoric acid, in the preparation of $VOHPO_4{\cdot}0.5H_2O$, a series of phases can be obtained starting with the pure $VOHPO_4{\cdot}0.5H_2O$ phase and leading ultimately to a new NH_3 incorporated phase containing mixed-valent vanadium. In between these two extremes a series of weakly crystalline (**P-4**) and amorphous phases (**P-5**, **P-6**) are formed which consist of the $VOHPO_4{\cdot}0.5H_2O$ phase and an X-ray amorphous V^{5+} phase containing bound NH_3 species. These phases undergo transformation to the pyrophosphate phase. Consequently, in view of the reported importance of V^{5+} species in the activity of the vanadium pyrophosphate phase for the selective oxidation of hydrocarbons, particularly butane, these phases could be strong candidates for selective oxidation catalysts. In particular, the formation of a pyrophosphate phase (which involves condensation of P–OH groups from adjacent layers of the orthophosphate) from amorphous phases containing $VOHPO_4{\cdot}0.5H_2O$ with NH_3 bound to P–OH groups could have important implications in the activity of the pyrophosphate since its microstructure (which is known to have a profound effect on its catalytic activity) would be quite different from a pyrophosphate phase obtained from the pure hemihydrate with free P–OH groups.

2. The *in-situ* generation of NH_3 during the use of hydroxylamine hydrochloride as a reductant for V_2O_5 is a very novel aspect of the chemistry of vanadium phosphates and provides a convenient method for the preparation of interesting NH_3 incorporated vanadium phosphate phases. These phases could have strong potential as ammoxidation catalysts since it is believed[19] that adsorbed NH_3 and NH_4^+ type species are responsible for O^- as well as N insertion reactions in the ammoxidation of methyl aromatics to the nitriles *via* aldehyde intermediates over vanadium phosphate catalysts.

Acknowledgement

One of the authors (S. D.) is grateful to the CSIR, New Delhi for the award of a Senior Research Fellowship.

References

1 G. Centi, F. Trifiro, J. R. Ebner and V. M. Franchetti, *Chem. Rev.*, 1988, **88**, 55.
2 G. Centi, *Catal. Today*, 1993, **16**, 5 and references therein.
3 T. Shimoda, T. Okuhara and M. Misono, *Bull. Chem. Soc. Jpn.*, 1985, **58**, 2163.
4 G. Busca, F. Cavani, G. Centi and F. Trifiro, *J. Catal.*, 1986, **99**, 400.
5 C. J. Kiely, A. Burrows, S. Sajip, G. J. Hutchings, M. T. Sananes, A. Tuel and J. C. Volta, *J. Catal.*, 1996, **162**, 31.
6 M. T. Sananes-Schulz, A. Tuel, G. J. Hutchings and J. C. Volta, *J. Catal.*, 1997, **166**, 388.
7 Y. Zhang, A. Martin, H. Berndt, B. Lücke and M. Meisel, *J. Mol. Catal., A: Chem.*, 1997, **118**, 205.
8 J. P. Joly, C. Mehier, K. E. Bere and M. Abon, *Appl. Catal., A: Gen.*, 1998, **169**, 55.
9 (*a*) A. Datta, A. R. Saple and R. Y. Kelkar, *J. Chem. Soc., Chem. Commun.*, 1991, 356; (*b*) A. Datta, A. R. Saple and R. Y. Kelkar, *J. Chem. Soc., Chem. Commun.*, 1991, 1645; (*c*) A. Datta, S. Bhaduri, R. Y. Kelkar and H. I. Khwaja, *J. Phys. Chem.*, 1994, **98**, 11811; (*d*) A. Datta, R. Y. Kelkar and A. R. Saple, *J. Chem. Soc., Dalton Trans.*, 1994, 2145.
10 A. R. Antonio, R. L. Barbour and P. R. Blum, *Inorg. Chem.*, 1987, **26**, 1235.
11 (*a*) R. Rajadhyaksha and H. Knozinger, *Appl. Catal., A*, 1989, **51**, 81; (*b*) G. Ramis, G. Busca, F. Bregani and P. Forzatti, *Appl. Catal.*, 1990, **64**, 259; (*c*) Y. Zhang, A. Martin, H. Berndt, B. Lücke and M. Meisel, *J. Mol. Catal., A: Chem.*, 1997, **118**, 205; (*d*) M. Inomata, A. Miyamoto and Y. Murakami, *J. Catal.*, 1980, **62**, 140.
12 A. Datta and R. Y. Kelkar, *Chem. Commun.*, 1996, 89.
13 M. Schraml-Marth, A. Wokaun and A. Baiker, *J. Catal.*, 1990, **124**, 86.
14 (*a*) J. Curilla and R. Datmansky, *Appl. Catal.*, 1988, **36**, 119; (*b*) J. G. Eon, R. Olier and J. C. Volta, *J. Catal.*, 1994, **145**, 318.
15 C. M. Flynn and M. T. Pope, *J. Am. Chem. Soc.*, 1970, **92**, 85.
16 M. Lopez Granados, J. C. Conesa and M. Fernandez-Garcia, *J. Catal.*, 1993, **141**, 671.
17 (*a*) Y. Zhang, A. Martin, G. V. Wolf, S. Rabe, H. Worzala, B. Lücke, M. Meisel and K. Witke, *Chem. Mater.*, 1996, **8**, 1135; (*b*) Y. Zhang, M. Meisel, A. Martin, B. Lücke, K. Witke and K. W. Brzezinka, *Chem. Mater.*, 1997, **9**, 1086.
18 J. W. Johnson and A. J. Jacobson, *Angew. Chem., Int. Ed. Engl.*, 1983, **22**, 412.
19 (*a*) H. Berndt, K. Buker, A. Martin, S. Rabe, Y. Zhang and M. Meisel, *Catal. Today*, 1996, **32**, 285; (*b*) G. Centi and S. Perathoner, *J. Catal.*, 1993, **142**, 84.